Electrodynamic Tether as a Thruster for MXER Studies

G. V. Khazanov[*], E.N. Krivorutsky[§], and K. Sorensen[†]

NASA Marshall Space Flight Center, Huntsville, Alabama, AL 35805

Electrodynamic propulsion based on the interaction of a conducting tether with the background magnetic field can be implemented across a range of system designs. Bare tethers, bare and insulated tethers with a balloon termination, and insulated tethers with a grid-sphere termination have been proposed for different applications. Electrodynamic tether as a thruster is currently proposed for the Momentum eXchange Electrodynamic Reboost (MXER) Tether System that is under development at NASA Marshal Space Flight Center. Different parameters describing tether performance, such as system acceleration and efficiency, can be calculated, if the current distribution along the tether at the satellite trajectory is known. We present the calculation of currents collected by the bare and partly insulated tethers with the circular (wire) and rectangular (tape) cross-sections operating in the thrust mode for MXER tether that is expected to operate in an equatorial elliptical orbit with perigee in the altitude range of 150-500km and apogee in the altitude range 5000-10000km. Collected current is calculated as a function of the satellite velocity and the Earth's magnetic field, plasma parameters (plasma density and temperature), and tether parameters (the length of the tether bare segment, the type and the dimensions of the cross-section). The deviation of the collected current from the OML model due to the tether geometry and self-induced magnetic field (for tether with a circular cross-section) is taken into account. We also present the calculation of the approximate range of current collection by a solid sphere and grid-sphere with the radius 10m.

Nomenclature

B_0 = ambient magnetic field

R = sphere (grid-sphere) radius

[*] Research Scientist, XD-12, 320 Sparkman Dr., Huntsville, AL 35805

[§] Research Scientist, XD-12, 320 Sparkman Dr., Huntsville, AL 35805.

[†] Electrical Engineer, In-Space Propulsion Technology Projects Office, 320 Sparkman Dr., Huntsville, AL 35805, Member AIAA.

c = speed of light

$\vec{E}$ = induced electric field

E_i = ion kinetic energy

E_m = induced electric field along the tether

e = elementary charge

G = geometrical correction coefficient to OML

I = current

I_0 = thermal current

I_{gs} = current collected by a grid-sphere

I_{ss} = current collected by a solid sphere

i = normalized current density

L^* = normalization length

l = normalized z-coordinate

m = electron mass

n_e = undisturbed electron density

p = tether perimeter

r = radial coordinate

r_b = boundary radius

r_w = wire radius

S = tether cross-section

T = temperature

$\vec{u}$ = satellite velocity

V^p = plasma potential

V^t = tether potential

V_R = sphere (grid-sphere) surface potential

V_b = boundary potential

ΔV = local bias

z = coordinate along the tether

w = tape width

x = normalized radial coordinate

α = grid-sphere transparency

λ_D = Debye length

ε = correction coefficient to OML due to magnetic shielding

σ = tether conductivity

ϕ = normalized tether bias

χ_b = normalized boundary potential

χ = normalized potential

1. Introduction

Electrodynamic propulsion based on the interaction of a conducting tether with the background magnetic field can be implemented across a range of system designs. Bare tethers,[1, 2] bare and insulated tethers with a balloon termination,[3 - 5] and insulated tethers with a grid-sphere termination [6] have been suggested for different applications.

An electrodynamic tether as a thruster is currently proposed for the Momentum-eXchange/Electrodynamic Reboost (MXER) tether facility that has the potential to provide a fully-reusable in-space propulsion infrastructure and dramatically reduce propulsion cost for many space missions.[7, 8]

In order for the tether system to boost multiple payloads, it must have a capability to restore its orbital energy and momentum after each payload transfer operation as rapidly as possible. The tether system that is positively-biased relative to the ambient environment require an anode contactor that will able it to collect electrons from ionospheric plasma. Because active plasma contactors require expenditure of propellant and may require significant additional mass, the bare wire tether technology is also being considered for the MXER tether.[9] The choice of a tether design for a specific mission is based on the analysis of tether system performance. Different parameters describing tether performance, such as system acceleration and efficiency, can be calculated, if the current distribution along the tether at the satellite trajectory is known. Below we present the results of current calculation along the expected trajectory of the MXER tether for wire and tape tethers with different cross-sections, and the approximate range of current collection by a solid sphere and grid-sphere with the radius 10m.

2. Tether current collection models

A. Models of current collection by wire and tape tethers

The basic physics of bare tether current collection is well known**.** The detailed formulation of the problem is presented in Ref. 1, 10 – 12. In the tether's reference frame of rest the electric field is $\vec{E} = \vec{u} \times \vec{B}_o / c$, where $\vec{u}$ is the tether orbital velocity, c is the speed of light, and B_0 is the ambient magnetic field. Below z-axe is chosen along the tether. The undisturbed potential, V^p , in plasma in the direction parallel to the wire is proportional to the projection of the electric field $\vec{E}$ on the tether direction, E_m , and $dV^p \sim E_m dz$. The potential along the wire, V^t , changes in accordance with Ohm's law. Then for the local bias we have $\Delta V = V^t - V^p$ and for the thruster mode the local bias changes as

$$\frac{d\Delta V}{dz} = \frac{I}{\sigma S} + E_m \tag{1}$$

where σ is the tether conductivity and S is the tether cross-section. The electrodynamics of a long conducting bare

or partly insulated tether is based on the OML theory of a cylindrical probe.[13] The equation for the OML current I along the tether is

$$\frac{dI}{dz} = en_e \varepsilon(l) G \frac{p}{\pi} \sqrt{\frac{2\Delta V}{m_e}} \tag{2}$$

Here: n_e is the unperturbed electron density; G and $\varepsilon(l)$ are the correction multiples accounting for the deviation from the standard OML theory due to large size and cross-section geometry of the tether (G) and the self-induced magnetic field ($\varepsilon(l)$); p is the tether perimeter. Both coefficients, $\varepsilon(l)$ and G are dependent on the system parameters, but the dependence on the tether length (local bias) in G can be neglected.[14, 15] It can be found from these papers that for a wire with the radius r_w, $r_w < \lambda_D, G = 1; r_w = 2\lambda_D, G = 0.97.$ For a tape with the width w, $w \le 4\lambda_D, G = 1; \quad w = 8\lambda_D, G = 0.97; \quad w = 12\lambda_D, G = 0.92; \quad w = 16\lambda_D, G = 0.8.$ Here λ_D is the Debye length. Calculation of $\varepsilon(l)$ is presented in Ref. 11. In the dimensionless variables

$$l = \frac{z}{L^*}; \quad L^* = \left(\frac{m_e E_m}{2e} \left(\frac{3\pi\sigma S}{4Gepn_e} \right)^2 \right)^{1/3}; \quad i = \frac{I}{\sigma S E_m}; \quad \phi = \frac{\Delta V}{E_m L^*} \tag{3}$$

equations (1) and (2) can be written as

$$\frac{di}{dl} = \frac{3}{4} \varepsilon(l) \sqrt{\phi}; \qquad \frac{d\phi}{dl} = i + 1 \tag{4}$$

The boundary condition for the current is $i_A = 0$ at the tether end A. It is also assumed that the potential at this point, $\phi_A = 0$, neglecting by its fluctuations in this preliminary consideration. Such approach essentially simplifies the system analyses and it is reasonable on this stage of MXER tether project. Because the solution of the equations is completely determined by the boundary conditions at point A, the results describe the fully bare tether as well as the partly insulated one.

B. Models of current collection by solid sphere and grid-sphere

For a solid sphere contactor we will assume that the region outside the sphere can be divided in two. The first region, starting from the sphere surface, is assumed to be spherically symmetrical with the Boltzmann ion

distribution and one-dimensionally accelerated electrons.[16, 17] The boundary of this region has the potential that reflects the flux of ions related to the satellite motion,[17, 18] and collects the current equal to the upper-limit current corresponding to the two-dimensional electrons acceleration found in Ref. 16. According to Ref. 16 this current, collected by the boundary of the first region, is:

$$\frac{I}{I_0} = \frac{1}{\sqrt{\pi}} \frac{r_b^2}{R^2} \left(\sqrt{\chi_b} + \frac{1}{2\sqrt{\chi_b}} \right) \tag{5}$$

where r_b is the boundary radius, $\chi_b = -eV_b / T$ (V_b is the potential of the boundary), and $I_0 = \pi R^2 e n_e \sqrt{\frac{8T}{\pi m}}$.

It is assumed in expression (5) that the current is collected only by the ram hemisphere. Following Ref. 17, 18 the potential at the boundary is taken equal to the energy needed to reflect the ions. It is defined by the normal component of the ion velocity relative to the satellite and averaged over the sphere surface, so $\chi_b = E_i / 3T$ and $E_i \approx 5\text{eV}$ is the ion kinetic energy.

To calculate the current from expression (5) the radius of the boundary, r_b, that separates the regions of one- and two- dimensional acceleration should be found. To calculate this boundary radius the Poisson equation in the region between the sphere surface and the boundary has been solved

$$\frac{1}{x^2} \frac{d}{dx} x^2 \frac{d\chi}{dx} = \frac{R^2}{\lambda_D^2} \left(\frac{2}{\sqrt{\pi\chi}} - e^{-\chi} \right), \; 1 \le x \le \frac{r_b}{R}. \tag{6}$$

The electron density here (the first term at the right-hand side of the equation) corresponds to the one-dimensional acceleration [16] with $\chi >> 1$. At the outer boundary of this region, r_b, the electron density is taken approximately equal to the ion density and because of the ion reflection it is taken two times larger than the undisturbed ion density.[17]

To calculate the boundary radius, r_b, from equation (6) three conditions are needed and, therefore, the Poisson equation should be solved in the domain $r > r_b$. To simplify the problem we assumed that the boundary between the regions of one- and two-dimensional acceleration approximately can be identified as the position, where the electric field abruptly changes. As can be expected from equation (6) it is also the radius where the potential, χ, is close to zero.

So, the boundary radius, r_b, has been defined as the point where the potential is close to zero and the electric field abruptly changes. Equation (6) has been solved starting from the sphere surface with the known potential and some potential derivative. The potential derivative on this surface has been adjusted until the point defined above as the boundary has been found. Starting from this point the assumed density distribution is not applicable. To verify the model, such calculations have been performed for a set of system parameters for which the experimental data are available. The results of calculations are in reasonable agreement with the measurements from TSS-1 and TSS-1R missions.[19]

We will also use the model presented above for the estimation of the upper bound of the current collected by the grid-sphere. For the estimation of the upper bound of the current collected by the grid-sphere we assumed that it is related to the current collected by the solid sphere as

$$I_{gs} = 4(1-\alpha)I_{ss} \tag{7}$$

Here I_{gs} is the current collected by the grid-sphere, I_{ss} is the current collected by the solid sphere, and α is the grid-sphere transparency, equal approximately to the ratio of the part of the sphere surface without the mesh to its total surface. It is assumed in equation (7) that the grid-sphere transparency is large, the electron crossing the grid-sphere will intersect its surface twice, and electrons crossing the wake hemisphere will be attracted back into the grid-sphere by the surface potential enlarging the collected current. For the current upper bound estimation current collected by the wake hemisphere is taken equal to the current collected by the ram hemisphere. In more details the models of current collection by a solid sphere and grid-sphere can be found in the Ref. 20.

3. Results

It is expected that the MXER tether would operate in an equatorial elliptical orbit with the perigee in the altitude range of 300-500km and the apogee in the range of 5000-10000km.[8] The specific orbit chosen would be a function of the tip velocity of the tether, which is in turn a function of the orbital transfer desired and the limitations of tensile material strength. The induced electric field for such a trajectory in the range of altitudes 300-900km is presented in Table 1. Table 1 also contains the typical plasma densities for day and night. The temperature is taken to be 1900º K. The angle between the satellite velocity and the Earth's magnetic field has been taken 90º in these calculations.

Table 1 Plasma parameters

H, km	B_0, G	E_m, V/km	n_e, cm^{-3}, day	n_e, cm^{-3}, night
300	0.27	230	$1.6 \cdot 10^6$	$1.0 \cdot 10^5$
400	0.26	220	$1.5 \cdot 10^6$	$3.0 \cdot 10^5$
500	0.25	210	$9.0 \cdot 10^5$	$2.0 \cdot 10^5$
700	0.23	190	$2.0 \cdot 10^5$	$8.0 \cdot 10^4$
900	0.21	170	$7.0 \cdot 10^4$	$3.0 \cdot 10^4$

The range of the cross-sections and the tethers length have been chosen taking into account the currents required for the MXER tether facility.

The current is calculated for the wires with the radiuses, r_w, equal 2.0mm, 2.5mm, and 3.0mm. For the same plasma parameters the current and local bias are also calculated for three tapes with the cross-sections presented in the Table 2, neglecting the self-induced magnetic field correction in equation (4). The self-induced magnetic field effect for the tape should be essentially smaller than for the wire because of the topology of the magnetic field around a tape. The same conclusion follows from the analyses presented in Ref. 12

Table 2 Tape parameters

Cross-section area, mm^2	Width, mm	Thickness, mm
4.0	20.0	0.2
4.0	40.0	0.1
6.0	60.0	0.1

Examples of the current and local bias distributions along the tether are presented in Fig.1. The length at these plots is the length of the bare part of the tether, counted from the end of the tether.

Currently investigated designs for the MXER tether facility requires large currents. Table 3 contains the tether length (L) and the voltage (V) needed for collection of current about 50A for tethers with different geometry (wire radius, r_w, and tape width, w) at different altitudes (H). Subscripts “d” and “n” corresponds to day and night. The tether length is restricted by 20km for the wire and by 10km for the tape.

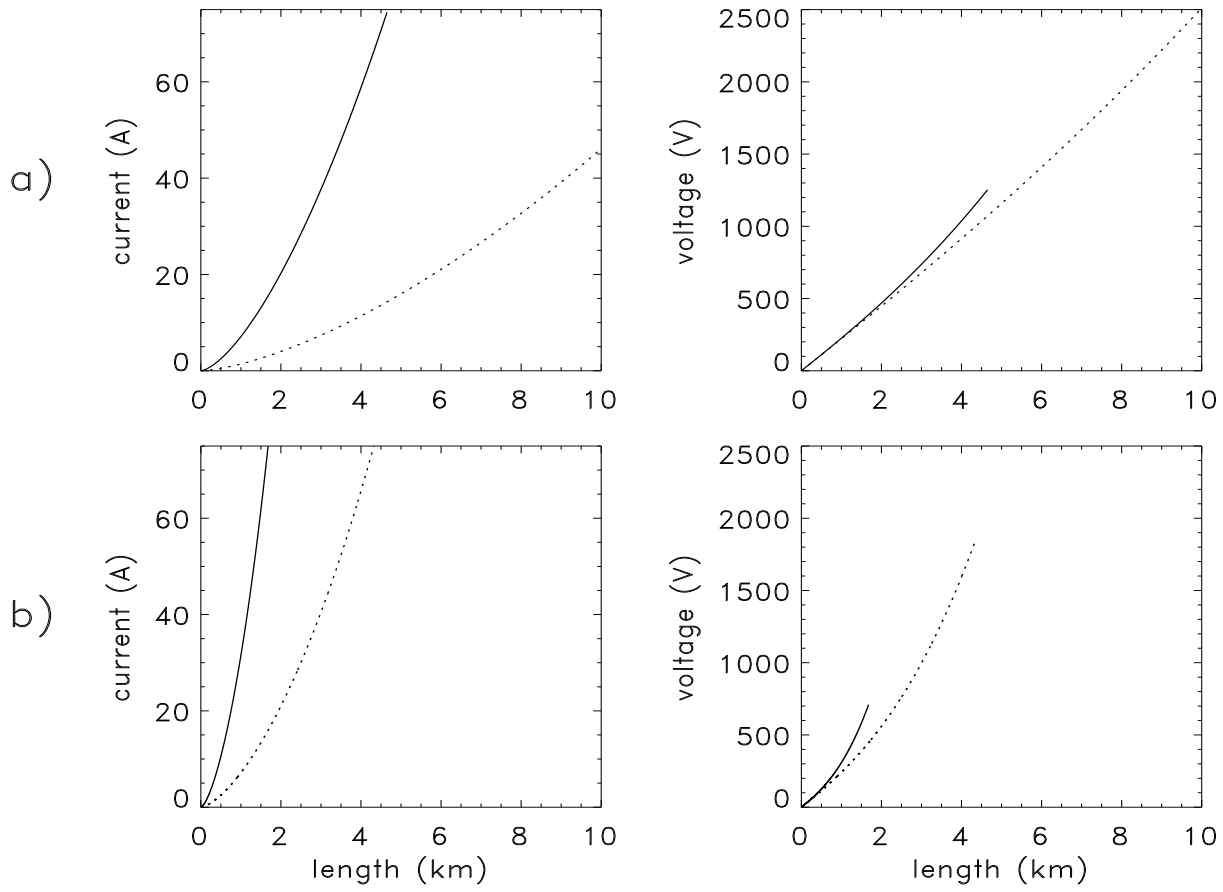

Fig. 1 Current and local bias distributions along the tether for the altitude 400km. Panel a) is for the wire with radius 2. 5mm; panel b) is for the tape with the cross-section 4mm^2 and the tape width 40mm. Solid and dotted lines are for day and night plasma densities respectively.

The approximate range of current collection by a solid sphere and grid-sphere with the radius 10m is presented in Table 4. Here we used the representative magnitudes for day and night plasma density and set the temperature equal 1eV. The grid-sphere transparency, α, is taken 0.9. The numbers in the nominator and denominator are the currents (in ampere) collected by the solid sphere and grid-sphere respectively.

Because the currents required for MXER tether operation are large and their magnetic fields are large compared to the ambient magnetic field in the vicinity of the tether we analyzed the role of magnetic shielding for the wire in some details.

Table 3 Results of calculation for wire and tape tethers

H, km	300			400			500			700			900	
r_w,mm	**2.0**	**2.5**	**3.0**	**2.0**	**2.5**	**3.0**	**2.0**	**2.5**	**3.0**	**2.0**	**2.5**	**3.0**	**2.5**	**3.0**
L_d,km	4.0	3.3	3.0	4.0	3.6	3.0	6.0	5.0	4.5	16.5	15.0	12.7	>20	>20
V_d,kV	1.1	0.9	0.8	1.1	0.9	0.75	1.6	1.2	1.05	4.0	3.3	2.6		
L_n,km	>20	>20	19	12.0	10.5	9.5	16.0	14.0	12.5	>20	>20	>20	>20	>20
V_n,kV			5.0	3.3	2.8	2.3	4.2	3.4	2.9					
w,cm	**2.0**	**4.0**	**6.0**	**2.0**	**4.0**	**6.0**	**2.0**	**4.0**	**6.0**	**2.0**	**4.0**	**6.0**	**4.0**	**6.0**
L_d,km	1.6	1.2	1.3	1.8	1.2	1.3	2.5	1.6	1.5	7.1	4.5	3.6	9.5	7.5
V_d,kV	0.6	0.45	0.4	0.65	0.45	0.4	0.8	0.6	0.45	2.2	1.4	1.0	2.9	2.0
L_n,km	>10	6.8	5.5	5.3	3.5	2.8	7.0	4.5	3.5	>10	8.4	6.5	>10	>10
V_n,kV		2.6	1.8	1.9	1.3	0.9	2.4	1.6	1.05		2.7	1.8		

Table 4 Currents collected

by solid sphere and grid-sphere

	V_R, V		
Ne,cm^{-3}	100	500	1000
$5 \cdot 10^4$	1.5/0.6	2.3/0.9	2.8/1.1
$7 \cdot 10^5$	19/7.5	21/8.4	23/9.2

As can be seen from equation (4) setting the coefficient $\varepsilon(l)$ equal to one eliminates the current's magnetic field from the calculations. Current found in this approximation is practically the same as presented above and the magnetic shielding is negligible for the equatorial elliptical orbit.[10 - 12, 19] It should be stressed that it is not always the case and essentially depends on the specific of the mission. If an inclined orbit for the MXER tether were to be used then the role of magnetic shielding can be not negligible. Figure 2 presents the current reduction for the thruster mode for a tether on a non-equatorial orbit. The angle between the tether and the ambient magnetic field in this case is taken not 90º, as in the calculations above, but 30º. As can be seen from the Figure 2 for such trajectory the effect of shielding is essential. The current is reduced by a factor of two for the tether with a bare length of 5km. The reason for such different role of magnetic shielding for these two orbits is discussed in Ref. 10 – 12, 19. Equatorial orbit is strongly favored for the MXER tether since it allows repeated rendezvous opportunities between the tether and payload in the event of a missed "catch".

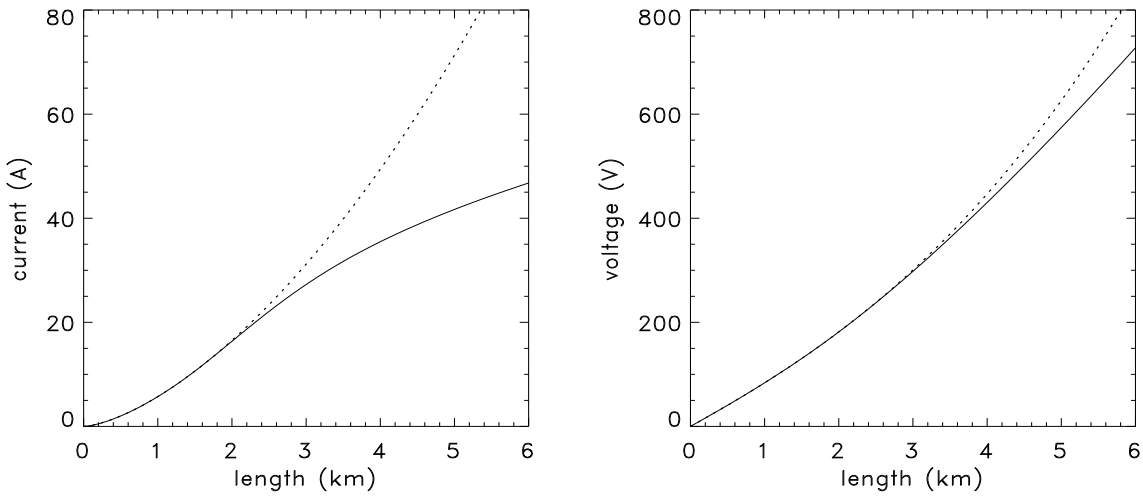

Fig. 2 Current and local bias distributions along the tether calculated with the magnetic shielding (solid lines), and neglecting it, for non-equatorial trajectory; r_w=2.5mm, n_e=2·10^{6}cm^{-3} , E_m=80V/km, B_0=0.25G.

3. Conclusion

We calculated the current that can be collected by wire and tape tethers (bare or partly insulated) along an equatorial elliptical orbit with the perigee in the altitude range of 300-500km and the apogee between 5000-10000km. Calculations are performed for the day and night conditions. Such orbital conditions are expected for the MXER tether operational concept. The current is calculated taking into account the corrections to the Orbit Limited Model that result from the size and the form of tether cross-section and magnetic shielding. It has been found that for the planned equatorial orbit the effect of magnetic shielding is negligible, while it can be essential for orbits with significant inclination. We also calculated currents that can be collected by a large (with 10m radius) solid sphere and grid-sphere contactors. Calculated results are covering a wide range of plasma and tether parameters along the planned MXER tether trajectory for different tether designs and can be used for the preliminary analyses of the tether performance and choice of the preferable technology for system restoration.

Acknowledgments. The work described in this paper was funded in part by the In-Space Propulsion Technology Program, which is managed by NASA's Science Mission Directorate in Washington, D.C., and implemented by the In-Space Propulsion Technology Office at Marshall Space Flight Center in Huntsville, Alabama under the Technical

Task Agreement M-ISP-04-37. The program objective is to develop in-space propulsion technologies that can enable or benefit near and mid-term NASA space science missions by significantly reducing cost, mass or travel times.

References

[1] Sanmartin, J. R., M. Martinez-Sanchez, and E. Ahedo, "Bare Wire Anodes for Electrodynamic Tethers," *Journal of Propulsion and Power*, Vol. 9, No. 3, 1993, pp. 353-360.

[2] Estes, R. D., E. C. Lorenzini, and J. R. Sanmartin, "Short Tethers for Electrodynamic Thrust," *Space Technology and Applications International Forum-2002*, edited by M. S. El-Genk, American Inst. of Physics, New-York, 2002, pp. 548-553.

[3] Vannarony, G., M. Dobrowolny, and F. De Venuto, "Deorbiting of LEO Satellites with Electrodynamic Tethers," AIAA Paper 2000-0328, 2000.

[4] Sanmartin, J. R., R. D. Estes, and E. C. Lorenzini, "Efficiency of Different Types of ED-Tether Thrusters," *Space Technology and Applications International Forum-2001*, edited by M. S. El-Genk, , American Inst. of Physics, New-York, 2001, pp. 479-487.

[5] Ahedo, E., and J. R. Sanmartin, "Analysis of Bare-Tether Systems for Deorbiting Low-Earth-Orbit Satellites," *Journal of Spacecraft and Rockets,* Vol. 39, No. 2, 2002, pp. 198-205.

[6] Stone N. H., J. D. Moore, W. R. Clayton, P. A. Gierow, "A Preliminary Assessment of Grid-Spheres Used as End-Body Electrodes for Electrodynamic Tether," *Space Technology and Applications International Forum-2002*, edited by M. S. El-Genk, American Inst. of Physics, New-York, 2002, pp. 537-547.

[7] Hoyt, R. P., "Design and Simulation of a Tether Boost Facility for LEO->GTO Payload Transport," AIAA Paper 2000-3866, *36th Joint Propulsion Conference*, July 2000.

[8] Sorensen K., "Momentum eXchange Electrodynamic Reboost (MXER) Tether," Technology Assessment Group Final Report, NASA MSFC, Huntsville, Alabama, 2003.

[9] Hoyt, R. P., J. T. Slostad, and S. S. Frank, "A Modular Momentum-Exchange/Electrodynamic-Reboost Tether System Architecture," AIAA Paper 2003-5214, *39th Joint Propulsion Conference*, July 2003.

[10] Khazanov G. V., N. H. Stone, E. N. Krivorutsky, and M. W. Liemohn, "Current-Produced Magnetic Field Effects on Current Collection," *Journal of Geophysical Research.*, Vol. 105, No. 7, 2000, pp. 15,835-842 .

[11] Khazanov G. V., N. H. Stone, E. N. Krivorutsky, K. V. Gamauynov, and M. W. Liemohn, "Current-Induced Magnetic Field Effects on Bare Tether Current Collection: A Parametric Study," *Journal of Geophysical Research*, Vol. 106, No. 6, 2001, pp. 10,565-579.

[12] Sanmartin, J. R. and R. D. Estes, "Magnetic Self-Field Effects on Current Collection by an Ionospheric Bare Tether," *Journal of Geophysical Research*, Vol. 107, No. 11, 10.1029/2002JA009344, 2002.

[13] Laframboise J. G., "Theory of Spherical and Cylindrical Langmuir Probes in Collisionless Maxwellian Plasma at Rest," University of Toronto, Institute of Aerospace Studies, Rept. No. 100, 1966.

[14] Sanmartin, J. R. and R. D. Estes, "The Orbital Motion Limited Regime for Cylindrical Langmuir Probes," *Physics of Plasmas,* Vol.6*,* No. 1, 1999, pp. 395-405.

[15] Estes, R. D., and J. R. Sanmartin, "Cylindrical Langmuir Probes Beyond the Orbital-Motion-Limited Regime," *Physics of Plasmas,* Vol. 7, No. 10, 2000, pp. 4320-4325.

[16] Laframboise, J. G., and L. W. Parker, "Probe Design for Orbit-Limited Current Collection," *Physics of Fluids,* Vol. 16, No. 5, 1973, pp. 629-636.

[17] Laframboise J. R., "Current Collection by a Positively Charged Spacecraft: Effects of its Magnetic Presheath," *Journal of Geophysical Research,* Vol. 102*,* No. 2, 1997, pp. 2417-2434.

[18] Cooke D. L., I. Katz, "TSS-1R Electron Currents: Magnetic Limited Collection from a Heated Presheath," *Geophysical Research Letters,* Vol. 25, No. 5, 1998, pp. 753-756.

[19] Khazanov, G. V., E. N. Krivorutsky, and K. Sorensen, "Analysis of Bare-Tether Systems as a Thruster for MXER Studies," *9th Spacecraft Charging Technology Conference,* Tsukuba, Japan, April 4-8, 2005.

[20] Khazanov, G. V., E. N. Krivorutsky, "Grid-Sphere Current Collection in View of the TSS-1, TSS-1R Missions Results," *Journal of Geophysical Research*, submitted, 2005.